E-Cadherin Mutational Landscape and Outcomes in Breast Invasive Lobular Carcinoma

Djerroudi, Lounes; Bendali, Amel; Fuhrmann, Laetitia; Benoist, Camille; Pierron, Gaelle; Masliah-Planchon, Julien; Kieffer, Yann; Carton, Matthieu; Tille, Jean-Christophe; Cyrta, Joanna; Ramtohul, Toulsie; Bonneau, Claire; Caly, Martial; Renault, Victor [**and 3 more**]

How to cite

DJERROUDI, Lounes et al. E-Cadherin Mutational Landscape and Outcomes in Breast Invasive Lobular Carcinoma. In: Modern pathology, 2024, vol. 37, n° 10, p. 100570. doi: 10.1016/j.modpat.2024.100570

This publication URL: https://archive-ouverte.unige.ch/unige:182881
Publication DOI: 10.1016/j.modpat.2024.100570

Mod Pathol 37 (2024) 100570

MODERN PATHOLOGY

USCAP UNITED STATES AND CANADIAN ACADEMY OF PATHOLOGY
Creating a Better Pathologist

Journal homepage: https://modernpathology.org/

Research Article

E-Cadherin Mutational Landscape and Outcomes in Breast Invasive Lobular Carcinoma

Lounes Djerroudi[a,b], Amel Bendali[a], Laetitia Fuhrmann[a], Camille Benoist[c], Gaelle Pierron[a], Julien Masliah-Planchon[a], Yann Kieffer[b], Matthieu Carton[d], Jean-Christophe Tille[a,e], Joanna Cyrta[a], Toulsie Ramtohul[f], Claire Bonneau[g], Martial Caly[a], Victor Renault[c], François-Clément Bidard[h], Fatima Mechta-Grigoriou[b], Anne Vincent-Salomon[a,*]

[a] *Institut Curie, Women's Cancer Institute, PSL University, Department of Diagnostic and Theranostic Medicine, Paris, France;* [b] *Institut Curie, Women's Cancer Institute, PSL University, INSERM U830, Stress and Cancer Laboratory, Paris, France;* [c] *Institut Curie, Women's Cancer Institute, PSL University, Clinical Bioinformatics, Paris, France;* [d] *Institut Curie, PSL University, Department of Statistics, Paris, France;* [e] *Hopitaux Universitaires de Geneve, Department of Pathology, Geneva, Switzerland;* [f] *Institut Curie, Women's Cancer Institute, PSL University, Department of Radiology, Paris, France;* [g] *Institut Curie, Women's Cancer Institute, Université de Versailles Saint-Quentin-en-Yvelines, Department of Surgery, Saint-Cloud, France;* [h] *Institut Curie, Women's Cancer Institute, Université de Versailles Saint-Quentin-en-Yvelines, Department of Medical Oncology, Saint-Cloud, France*

ARTICLE INFO

Article history:
Received 4 December 2023
Revised 21 June 2024
Accepted 11 July 2024
Available online 16 July 2024

Keywords:
CDH1 mutations
E-cadherin immunohistochemistry
invasive lobular carcinoma
prognosis

ABSTRACT

Invasive lobular carcinomas (ILC) are characterized by the loss of E-cadherin expression and *CDH1* gene inactivation. Diagnostic reproducibility for this tumor type is currently suboptimal and could be improved by a better understanding of its histomolecular and clinical heterogeneity. We have analyzed the relationship between the presence, type, or position of *CDH1* mutations, E-cadherin expression, and clinicopathological features (including outcome) in a retrospective series of 251 primary ILC with a long follow-up (median: 9.5 years). The mutational status of E-cadherin gene (*CDH1*) was determined by RNA sequencing from frozen tumor samples. E-cadherin immunohistochemistry (IHC) was performed with antibodies directed against the intracellular domain (clone 4A2C7) and the extracellular domain (clone NCH38). IHC expression of p120 and β-catenin was also assessed in E-cadherin diffusely positive cases. Three major patterns of E-cadherin membrane expression were identified by IHC, with good agreement between the 2 clones (overall concordance: 83.8%, Kappa 0.67): null/focal expression ($\leq$10%) (72.8% of cases for 4A2C7 and 83.8% for NCH38), heterogeneous expression (11%-89%) (19.2% of cases for 4A2C7 and 6.9% for NCH38), and diffuse expression ($\geq$90%) (8% of cases for 4A2C7 and 9.3% for NCH38). E-cadherin membranous expression, when present, was abnormal (incomplete labeling and/or reduced intensity). ILC with diffuse E-cadherin expression showed abnormal β-catenin or p120-catenin staining in 21% of cases. Interestingly, these cases with diffusely expressed E-cadherin had a *CDH1* mutation rate as high as the E-cadherin null/focal cases (~70%) but were enriched in nontruncating mutations. Regarding *CDH1* mutation location, intracytoplasmic domain mutations correlated with a divergent E-cadherin IHC phenotype between the 2 antibodies (4A2C7 $\leq$ 10%/NCH38 $\geq$ 10%). Clinico-pathological correlation analyses found that stromal amount (inversely correlated with tumor cellularity) and tumor-infiltrating lymphocytes were less abundant in ILC with E-cadherin null/focal cases. In addition, *CDH1* truncating mutations were associated with radiohistologic size discordance and were identified in multivariate survival analysis as an independent poor prognosis factor in terms of metastasis risk and breast cancer-related mortality. Overall, our study highlights the importance of the precise mutational status of *CDH1* in the clinical, radiological, histologic, and

* Corresponding author.
E-mail address: anne.salomon@curie.fr (A. Vincent-Salomon).

https://doi.org/10.1016/j.modpat.2024.100570

phenotypic expression of lobular carcinomas. These findings should be taken into account in future attempts to improve diagnostic criteria or methods for ILC, as well as for clinicobiological studies dedicated to this tumor type.

Introduction

Invasive lobular carcinoma (ILC) is the second most common histological type of breast cancer, accounting for 15% of all breast carcinomas. It is characterized by dyscohesive tumor cells, related to E-cadherin inactivation.[1] Despite being a well-established histopathological entity for several decades, recent studies have raised questions about the reliability and reproducibility of ILC diagnosis. Central histology reviews of 2 major trials[2,3] published in 2020 revealed that the diagnosis of ILC was confirmed in only 2/3 of cases. Inconsistencies in ILC diagnosis may be due to several factors, linked not only to the variability of diagnostic methods in use but also to the complexity of the disease itself.[4]

De Schepper et al[5] have recently shown that there is considerable heterogeneity in diagnostic practices concerning ILC. The variability of laboratory methods includes the use or nonuse of E-cadherin immunohistochemistry (IHC), as well as the clone used: some targeting the extracellular domain of E-cadherin (including NCH38, the most commonly used clone worldwide) and other clones targeting the intracellular part of the protein (including the 4A2C7 clone). Standardization of practices could improve the reliability of ILC diagnosis, as previously shown for the systematic use of E-cadherin IHC[4] (not mandatory according to current World Health Organization recommendations).

The histomolecular heterogeneity of ILCs further increases diagnostic complexity. Although classic ILC (composed of dyscohesive tumor cells dissociated or arranged in single files) associated with E-cadherin inactivation is the typical form of this disease, several morphologic, phenotypic, and molecular types have been described.[1,6-8] The World Health Organization histologic classification currently identifies different ILC subtypes, depending on tumor architecture (solid, alveolar, etc.) or cytology (pleomorphic, apocrine, etc.). Phenotypically, over 90% of ILCs are luminal, but a small subset are HER2-positive.[7,8] Some rare triple-negative ILCs have also been described, being frequently pleomorphic and belonging to the luminal androgen receptor molecular group.[9] Inactivation of *CDH1* (the gene encoding E-cadherin) occurs in about two-thirds of cases by mutation (>85% of truncating type), associated with loss of the other allele.[6,10-13] Notably, large molecular studies using sensitive techniques consistently report a significant subset of ILCs without detectable *CDH1* mutations, but for which histophenotypic data are very scarce. At the protein level, although E-cadherin is absent in most ILCs, it has been reported that 10% to 15% of cases maintain immunohistochemical expression of E-cadherin but that the expression pattern is often abnormal.[14,15]

To date, little is known about the links between the presence, type, and localization along the gene sequence of *CDH1* mutations, and the expression pattern of E-cadherin, the morpho-phenotypic tumor characteristics, and the clinical course of ILCs. These data are crucial to better understand this disease and improve our diagnostic accuracy, especially in the current context of emerging therapies that can specifically target ILC.[8,16,17]

In that context, the aims of our study were as follows: first, to correlate the mutational landscape of *CDH1* gene with E-cadherin expression determined by IHC using 2 clones, NCH38 targeting extracellular E-cadherin domain and 4A2C7 targeting intracytoplasmic domain; second, to correlate E-cadherin status with histopathological features of ILC; and third, to determine the prognostic impact of mutational status of *CDH1* and E-cadherin expression in a large series of 251 ILCs from the Institut Curie.

Materials and Methods

Patients and Samples

The study was based on a series of 251 patients who consecutively underwent surgery at Institut Curie for a primary ILC (prior to any treatment) between 2005 and 2008 and for whom frozen tumor samples were available for RNA sequencing. This series was part of a previously described larger cohort.[18] Histopathological review of the cases was done in accordance with current standards by experienced breast pathologists (J.C.T., A.V.S., and L.D.), as previously reported.[18] Tumor cellularity was determined microscopically as the proportion of tumor cells among all cell types. Mammographic or ultrasound tumor size was collected and used to evaluate radiohistological size concordance. Survival data of patients were also collected, with a median follow-up of 9.5 years (range: 0.3-15.0 years). Informed patient consents were recorded for using tissue samples for research purposes. This study has been approved by our institutional review board.

Immunostaining

The staining processes and evaluation methods were described elsewhere.[18] In brief, 3-μm thick formalin-fixed paraffin-embedded sections were mounted on slides and stained as recommended by current guidelines[19-21] with antibodies directed against ER (clone 6F11, Novocastra; 1:200 dilution), progesterone receptor (PR) (clone 1A6, Novocastra; 1:100 dilution), HER2 (clone CB11, Novocastra; 1:100 dilution), the intracellular part of E-cadherin (clone 4A2C7, Invitrogen; 1:100 dilution), the extracellular part of E-cadherin (clone NCH38, Agilent Technologies; 1:100 dilution), β-catenin (clone 14, BD Biosciences; 1:200 dilution), and p120-catenin (clone D7S2M, Cell Signaling Technology; 1:400 dilution).

Assessment of E-cadherin staining with both clones was performed as follows: (1) evaluation of staining intensity in normal glands; (2) absence or presence of staining on ILC cell membrane, cytoplasm, or nucleus; (3) if membranous staining was present: assessment of its complete or incomplete pattern; and (4) determining the staining intensity and the percentage of positive cells. In this article, unless otherwise stated, only membrane and cytoplasmic expression were taken into account when referring to the overall percentage of cells labeled by E-cadherin antibodies.

For hormone receptor assessment, a threshold of 10% for ER/PR positivity was applied according to the *Groupe d'étude des facteurs pronostiques immunohistochimiques dans le cancer du sein* guidelines.[22,23] Assessment of HER2 status was performed following

ASCO/CAP recommendations.[19] Histomolecular subtypes were defined as follows: luminal A—ER ≥10% and either mitotic score of 1 or mitotic score 2 associated with PR ≥ 20%; luminal B—ER ≥10% and either mitotic score of 3 or mitotic score of 2 associated with PR <20%; HER2—HER2-positive, regardless of hormone receptor status; triple-negative—ER-negative (<10%), PR-negative (<10%), and HER2 not amplified.[24,25]

RNA Sequencing Analyses and Mutational Status Determination

The mutational profile of *CDH1* was determined by RNA sequencing of the 251 ILC. At our institute, RNAseq is routinely performed to characterize patient tumors in multiple molecular aspects (mutation, translocation, and expression data) using a small amount of the tumor sample. This technique is both highly informative and material-saving and offers an advantage for small diagnostic samples. In the context of our research project, the use of RNAseq on all cases in our ILC series (instead of DNAseq) allowed us to maximize the amount of information obtained from a single tumor fragment analysis (including the possibility of obtaining both mutational and biological information on tumors from a single sequencing run). To do so, total RNA from tumors was extracted and subjected to deoxyribonuclease treatment (Nucleospin miRNA deoxyribonuclease, Macherey-Nagel). Overall, 500 ng of good-quality RNA with a majority of samples showing RIN >7 (Bio-Analyzer, Agilent) were employed for Illumina library preparation using the Illumina TruSeq Stranded Total RNA Prep kit, which allows us to account for strand information. In the first step of ribodepletion, the RiboZero Gold kit was applied so as to eliminate both cytoplasmic and mitochondrial ribosomal RNAs. After fragmentation, cDNA synthesis was carried out, with the resulting fragments used for dA-tailing. This was followed by ligating TruSeq dual-index adapters. PCR amplification was eventually achieved with 13 cycles able to generate the final barcoded cDNA libraries. Libraries were equimolarly pooled and subjected to quantitative PCR quantification using the KAPA library quantification kit (Roche). Sequencing was carried out on the NovaSeq 6000 instrument from Illumina based on a 2 × 100 cycle mode (paired-end reads, 2 × 100 bases) to obtain around 100 million clusters (200 million raw paired-end reads) per sample. Fastq files were generated from raw sequencing data after demultiplexing based on barcode sequences using bcl2fastq. Expression data were generated with SALMON (v0.13.1) on ensembl96 (hg19), with the count matrix normalized to transcripts per million using tximport (R library). Read alignment was performed with STAR (v2.5.3a, on hg19 reference genome). Read cleaning was conducted in line with genome analysis toolkit (GATK) good practices (v3.5) for marking duplicates, base recalibrations, and indel realignments. The presence of the variant was inferred from RNAseq data, using a bioinformatic pipeline developed in our institute for diagnosis purposes. Variant calling was performed on *CDH1* gene using Haplotype Caller (GATK v.3.5) and Mutect2 (GATK v.4). Reads with mapping quality lower than 6, as well as sequenced bases quality lower than 20, were not considered for the variant calling. Variants were annotated with ANNOVAR (v2018Apr16) while being formatted with the Python package hgvs (v1.2.5). Intra- and inter-analysis of variant occurrence was applied to eliminate noise from the sequencing technology. Overall, only nonsynonymous mutations with an allelic ratio ≥5% and depth of coverage ≥10 (with at least 5 reads carrying the alternative allele), in addition to a ≤0.01% frequency in population databases and ≤10% internal Curie database, were eventually retained. For missense mutations not referenced as hotspots, only mutations with a "deleterious" prediction score for at least 2 of 10 prediction tools were retained. Mutations known to be hotspots were systematically retained. Each selected variant was validated using visualization in Integrated Genomics Viewer,[26] with annotations rechecked as necessary using either VarSome[27] or Alamut Visual Plus (Sophia Genetics). Mutations were classified as follows: truncating mutations (frameshift indels, stop-gain, stop-loss, or splice site mutations), missense mutations, and in-frame mutations (in-frame indels). If the mutations could not fit into any of these categories, they were classified as "other." Since RNA sequencing is not a standard technique for the mutational characterization of tumors, we validated RNAseq-based *CDH1* mutation identification by targeted DNA sequencing (using an in-house gene panel[28] including the *CDH1* gene) for 110 cases with available DNA.

Statistical Analyses

Baseline characteristics were expressed as frequencies and percentages for qualitative data, as well as mean, SD, and range for continuous variables. Associations between categorical variables were evaluated using chi-squared or Fisher exact tests, as appropriate. For continuous variables, Student *t* test or Wilcoxon rank-sum tests (Mann-Whitney) were applied, considering the normality of the distribution. The comparison of E-cadherin staining from clones 4A2C7 and NCH38 was done via Cohen's κ values and overall agreement estimation. Breast cancer-specific survival (BCSS) was defined as the time from breast cancer diagnosis until the date of death from breast cancer. Patients still alive were censored at the date of the last news. Distant metastasis-free interval (DMFI) was defined as the interval from breast cancer diagnosis until the first distant recurrence. Patients with no distant recurrence were censored at the date of the last news. BCSS and DMFI were estimated using the Kaplan–Meier method, with comparisons between *CDH1* subgroups made using log-rank testing. Univariate and multivariate Cox analyses were additionally employed to evaluate the prognosis value of these subgroups. Variables that were significantly associated with survival in univariate analysis were included in the multivariate model. For all analyses, a *P* value ≤.05 was considered statistically significant.

Results

Mutational Status of the CDH1 Gene

Mutational profiling of the *CDH1* gene was carried out in a series of 251 primary ILCs (see Table 1 for detailed clinicopathological characteristics of the cohort). Analysis based on RNAseq data identified 180 *CDH1* variants (listed in Supplementary Table S1): 56 stop-gain mutations (31.1%), 47 frameshift insertions (26.1%), 55 frameshift deletions (30.6%), 4 in-frame deletion (2.2%), 15 missense mutations (8.3%), and 3 splicing mutations (1.7%). Detection of splicing mutations by RNAseq could be related to sequencing of unspliced RNAs or DNA fragments remaining after the RNA extraction step (very low amounts, as quality controls indicate high RNA purity after extraction). Using the transcriptomic sequences, we categorized the 3 splicing mutations as truncating mutations. Three cases harbored a double mutation of *CDH1* (in each case, one being truncating, and the other nontruncating). Thus, at a per-patient level, 161/251 cases (64.1%) demonstrated a *CDH1* truncating mutation (frameshift indels, nonsense, or splicing mutations), 16/251 cases (6.4%) only a

Table 1
Clinical and pathologic features of a series of 251 ILCs

Characteristic	Patients	
	No.	%
Age (y)		
<50	53	21.1%
50-64	104	41.4%%
≥65	94	37.5%
Menopausal status		
Premenopausal	72	29.6%
Postmenopausal	171	70.4%
Missing	8	
Histologic subtype		
Classic	170	67.7%
Alveolar	4	1.6%
Pleomorphic	10	4.0%
Solid	1	0.4%
Mixed	66	26.3%
Apocrine morphology		
No	237	94.4%
Yes	14	5.6%
pT(m)		
Unifocal	195	77.7%
Multifocal	56	22.3%
Tumor Size		
pT1a	2	0.8%
pT1b	38	15.1%
pT1c	114	45.4%
pT2	76	30.3%
pT3	21	8.4%
Nodal status		
pN0	175	69.7%
pN1	51	20.3%
pN2	18	7.2%
pN3	7	2.8%
Grade		
1	7	2.8%
2	207	82.5%
3	37	14.7%
Lymphovascular invasion		
No	224	89.2%
Yes	27	10.8%
Estrogen receptor		
Negative (<10%)	9	3.6%
Positive (≥10%)	242	96.4%
Progesterone receptor		
Negative (<10%)	63	25.1%
Positive (≥10%)	188	74.9%
HER2 status		
HER2-zero	159	63.3%
HER2-low	84	33.5%
HER2-positive	8	3.2%
Histomolecular class		
Luminal A	171	68.1%
Luminal B	63	25.1%
Luminal B/HER2	8	3.2%
Triple negative	9	3.6%
Tumor infiltrating lymphocytes		
<5%	182	72.5%
≥5%	69	27.5%
Tumor cellularity		
<50%	146	58.2%
≥50%	105	41.8%
Histo/radiological Size Ratio >1.5		
No	144	64.6%
Yes	79	35.4%
Missing	28	
Surgery		
Tumorectomy	168	66.9%
Mastectomy	83	33.1%
Radiotherapy		
No	22	8.8%
Yes	229	91.2%
Chemotherapy		
No	187	74.5%
Yes	64	25.5%
Hormone therapy		
No	35	13.9%
Yes	216	86.1%
Metastatic relapse		
No	212	84.5%
Yes	39	15.5%
Death from breast cancer		
No	230	91.6%
Yes	21	8.4%

ILC, invasive lobular carcinoma.

nontruncating mutation (in-frame indels or missense mutations), and 74 cases (29.5%) no detectable *CDH1* mutation. The average allelic ratio of *CDH1* mutations was 62.2%. The OncoKB database[29,30] listed 88.9% of the *CDH1* mutations identified in our series. DNA sequencing of 85 *CDH1*-mutated cases validated 84 of the 86 *CDH1* variants (97.7%) identified by RNAseq. DNA sequencing of 25 cases with no *CDH1* mutation detected by RNAseq found no *CDH1* mutation in 23 of 25 cases (92%). Of note, one of the 2 additional mutations found by DNAseq was actually found by RNAseq but had been filtered out due to insufficient coverage. The sensitivity of RNAseq vs DNAseq for the detection of *CDH1* mutations was 97.7%, specificity 92%, and accuracy 96.4%.

As expected, mutations were distributed throughout the *CDH1* gene (Fig. 1): 48 were in the propeptide/signal domain (26.7 %), 106 in the extracellular domain (58.9 %), 6 in the transmembrane domain (3.3 %), and 20 in the intracytoplasmic domain (11.1 %). In terms of recurrent mutations, defined as being present in at least 2 different cases in the series, we have identified: Q23* mutation (14 occurrences), T115Nfs*53/Afs*52 mutation (4 occurrences), 6 mutations with 3 occurrences (V202Cfs*7, D290Gfs*3/Rfs*2/Tfs*4, Q383*, Q610*, Q699*, and Y753Lfs*4), and 24 other mutations with 2 occurrences.

Immunohistochemical Expression of E-Cadherin Assessed With Clone 4A2C7 (Intracellular) and Clone NCH38 (Extracellular)

E-cadherin expression was assessed by immunohistochemistry with 2 different clones: one targeting the intracellular part of the protein (clone 4A2C7) and the other targeting the extracellular part (NCH38). Overall, 47.6% and 53.8% of ILCs showed no expression with 4A2C7 and NCH38 clones, respectively. Focal expression (1%-10% labeled cells) was observed in 25.2% and 30% of cases, heterogeneous expression (11%-89% labeled cells) in 19.2% and 6. 9% of cases, and diffuse expression (≥90% labeled cells) was observed in 8% and 9.3% of cases with 4A2C7 and NCH38, respectively (Fig. 2, Table 2). Considering a 3-class categorization of E-cadherin IHC (null/focal [≤10%], heterogeneous [11%-89%], and diffuse [≥90%]), the overall agreement between the 2 clone analyses was 83.8% and the Kappa was 0.67 (Supplementary Table S2). There was a

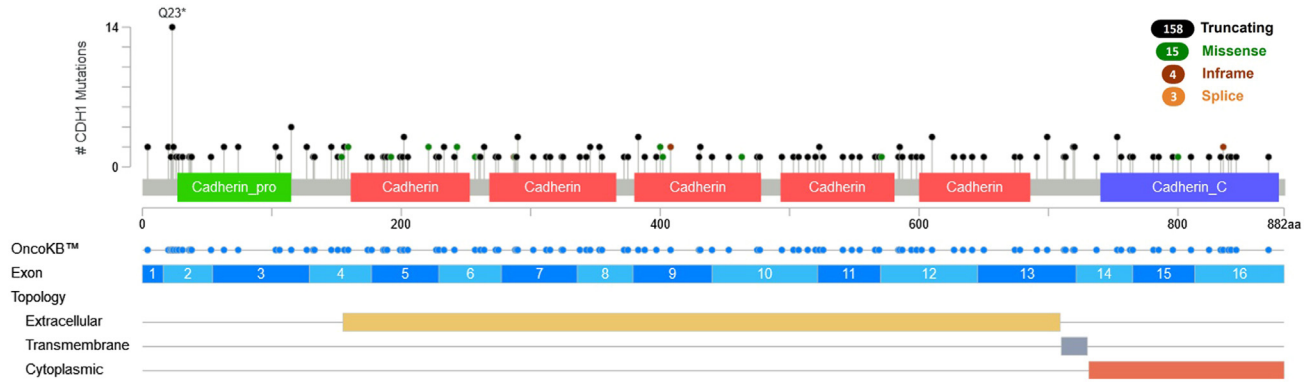

Figure 1.
CDH1 mutations are found all along the gene sequence and are mostly truncating (black).

significant correlation between RNA expression and protein expression of E-cadherin, with both clones (Supplementary Figs. S1 and S2). Expression of E-cadherin, when present, was membranous in almost all cases with frequent coexisting perimembranous cytoplasmic expression. E-cadherin expression was only cytoplasmic in 2 cases (including 1 case with a dot-like pattern) for clone 4A2C7 and in 1 case for clone NCH38. Nuclear expression of E-cadherin (in ≥10% of cells) was observed in 27 cases with the 4A2C7 antibody (19 cases with null/focal E-cadherin membrane expression and 8 cases with heterogeneous membranous expression) and 8 cases with the NCH38 antibody (7 cases with null/focal E-cadherin membranous expression and 1 case with heterogeneous membranous expression). The presence of E-cadherin nuclear expression was significantly associated with nondiffuse E-cadherin membrane labeling ($P < .001$, for both clones).

Notably, cases with diffuse E-cadherin expression had a decreased H-score (<300) in 19/20 cases for 4A2C7 (mean H-score: 241.7) and in 22/23 cases for NCH38 (mean H-score: 209.6); most cases also exhibited a discontinuous abnormal membrane staining (17/20 for 4A2C7 and 18/23 for NCH38) (Table 2). Of note, 4/23 cases with diffuse (≥90%) NCH38 E-cadherin showed null/focal (N = 1) or heterogeneous (N = 3) 4A2C7 E-cadherin labeling, whereas all diffuse 4A2C7 E-cadherin cases also showed diffuse labeling with the NCH38 clone (19/19 cases). β-catenin and p120-catenin immunohistochemistry was performed on 19 cases with a diffuse expression of E-cadherin with both clones 4A2C7 and NCH38. One case showed a strong reduction in membranous β-catenin expression (5% of labeled cells); this case harbored a mutation in the intracytoplasmic domain of *CDH1*. One case had more than 50% of cells with cytoplasmic p120-catenin expression, and 2 cases had a significant reduction (<50%) in membranous p120-catenin expression (Table 3).

Association Between E-Cadherin Expression, CDH1 Mutational Status, and Clinico-Pathological Features

Cases with *CDH1* truncating mutations were E-cadherin null/focal (0%-10% of stained cells) in 77.5% (124/160) of cases with clone 4A2C7 and in 89.9% (142/158) of cases with clone NCH38. Marked reduction in E-cadherin expression was also found at a similar rate in cases without *CDH1* mutations, with 75.7% (56/74) of E-cadherin null/focal with clone 4A2C7 ($P = .74$) and 86.3% (63/73) of E-cadherin null/focal with clone NCH38 ($P = .5$). In addition, the percentage of cases without *CDH1* mutations was distributed almost equally between ILC with diffuse (≥90%) vs null/focal (≤10%) E-cadherin expression (30% vs 31% for 4A2C7 and 35% vs 30% for NCH38, respectively). The presence of *CDH1* nontruncating mutations was significantly correlated with diffuse E-cadherin expression (≥90%) either with NCH38 or 4A2C7 antibodies ($P < .0001$) (Fig. 3A). The allelic ratio of *CDH1* mutations showed no statistically significant variation between E-cadherin null, focal, heterogeneous, or diffuse IHC categories. Cases with diffuse E-cadherin expression had no mutations involving the propeptide/signal domain (Fig. 3B). Analysis of discordant cases for intracellular (4A2C7) vs extracellular (NCH38) labeling showed that cases with both 4A2C7 ≤10% and NCH38 ≥10% were associated with enrichment in mutations of the intracytoplasmic domain of *CDH1* ($P < .01$) (Fig. 3C).

A high E-cadherin expression correlated with a lower tumor cellularity ($P < .01$ for 4A2C7 and $P < .05$ for NCH38) and a higher tumor-infiltrating lymphocytes (TILs) content ($P = .17$ for 4A2C7 and $P < .05$ for NCH38). CLI with null/focal E-cadherin labeling (≤10%) showed more radiohistologic discordance of tumor size (histological size/radiological size ratio >1.5) than the other groups ($P < .01$ for 4A2C7 and $P = .05$ for NCH38) (Supplementary Tables S3 and S4). The presence of a radiohistological discordance was also significantly associated with the group of tumors with a truncating mutation of *CDH1* ($P < .01$). Cases without *CDH1* mutation more frequently showed apocrine morphology ($P < .05$) (Supplementary Table S5).

Prognostic Impact of E-Cadherin Status in Invasive Lobular Carcinoma

Patients who had ILC with *CDH1* truncating mutation showed a shorter DMFI (Kaplan Meier analysis; log-rank test, $P < .01$) and a poorer BCSS (log-rank test, $P < .05$) than patients who had ILC without *CDH1* truncating mutation (including cases with *CDH1* nontruncating mutations and cases without *CDH1* mutations) (Fig. 4A, B, respectively). Patients who had ILC with *CDH1* truncating mutation experienced a 10-year DMFI of 78.1% (95% CI: 71.0%-85.8%) and a 10-year BCSS of 88.6% (95% CI: 82.8%-94.8%) compared with 95.7% (95% CI: 91.0%-100%) and 97.5% (95% CI: 94.0%-100%) for patients who had ILC without *CDH1* truncating mutations, respectively. This corresponds to a 17.6% difference for DMFI and 8.9% difference for BCSS, at 10 years. Of note, the poor prognosis associated

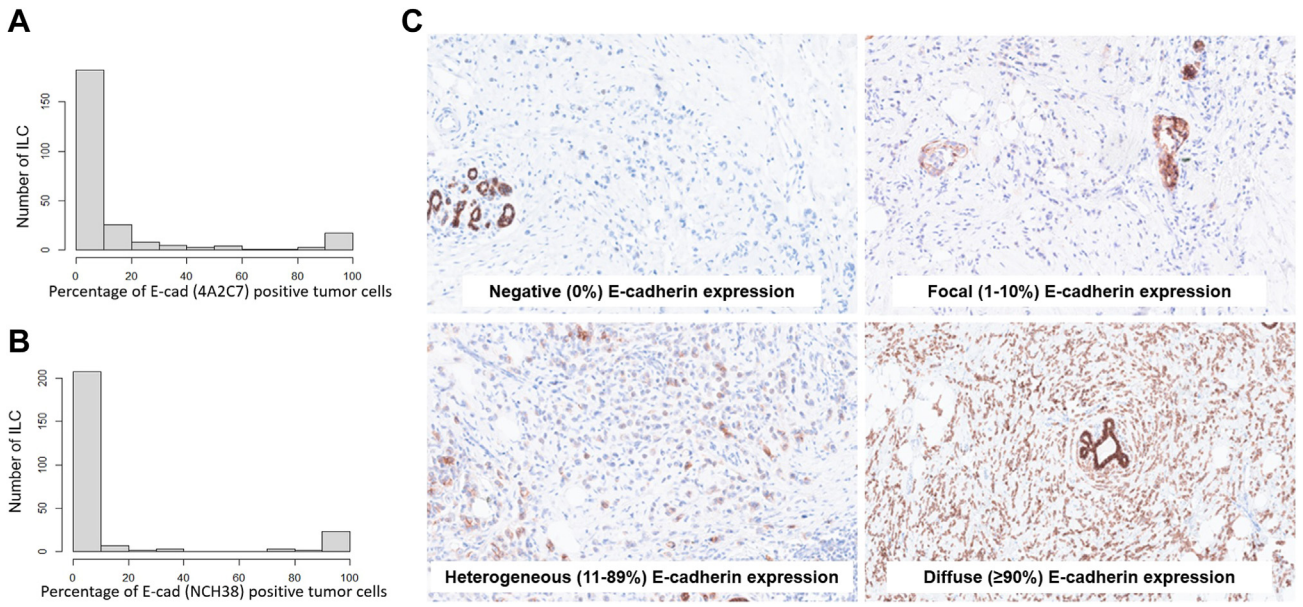

Figure 2.
Expression of E-cadherin across the invasive lobular carcinoma cohort. Distribution of E-cadherin membranous/cytoplasmic expression assessed with intracellular clone (4A2C7) (A) and extracellular clone (NCH38) (B). (C) Representative E-cadherin expression patterns are identified.

with *CDH1* truncating mutation was also found when analyses were restricted to E-cadherin null/focal (IHC ≤10%) ILCs, whether for DMFI (log-rank tests, $P < .01$ with clone 4A2C7, and $P < .05$ with clone NCH38) or BCSS (log-rank tests, $P < .05$ with clone 4A2C7 and with clone NCH38).

Univariate Cox proportional hazards analysis showed an increased risk of metastatic relapse (hazard ratio (HR) = 3.9, $P < .05$) and breast cancer-related death (HR = 4, $P = .06$) in the group of patients who had ILC with *CDH1* truncating mutation compared with patients who had ILCs without *CDH1* mutation. A moderate and nonsignificant increase in metastatic risk and breast cancer-related death was found for cases with *CDH1* nontruncating mutations (HR = 2.3, $P = .34$; HR = 2.3, $P = .50$, respectively). Features otherwise significantly associated in univariate analysis with metastatic risk were tumor size, lymph node status, and grade; features significantly associated with risk of breast cancer-related death were tumor size, lymph node status, PR status, and TILs (Table 4). Treatment characteristics (including type of surgery and use of radiotherapy, hormone therapy, or chemotherapy) had no effect on survival for either DMFI or BCSS. Of note, E-cadherin IHC was not associated with prognosis in our cohort, and in particular, no survival impact was found for nuclear E-cadherin positivity with both clones.

The poor prognostic value of *CDH1* truncating mutation was independent of tumor size, nodal status, grade, PR status, and TILs in multivariate analysis. HR values were 5.2 and 4.93 in the group of patients who had ILC with *CDH1* truncating mutation for DMFI and BCSS models, respectively ($P < .01$ and $P < .05$), in contrast with the lower HR values found in univariate models (Table 4). In addition, the inclusion of treatment variables in the multivariate model showed that the prognostic impact of *CDH1* mutation status (HR = 5.59, $P < .01$ for DMFI; HR = 4.61, $P = .05$ for BCSS) was independent of the type of surgery and the use of radiotherapy, hormone therapy, or chemotherapy.

Discussion

In this retrospective series of ILCs from a single institution with a long follow-up, we showed that ILCs diffusely expressing

Table 2
Characteristics of E-cadherin immunohistochemistry assessed with 2 antibodies: clone 4A2C7 targeting the intracellular part of the protein and clone NCH38 targeting the extracellular part

	4A2C7 clone	NCH38 clone
No. of ILCs assessed (/251)	250	247
Pattern of E-cadherin expression		
Negative (0%)	119 (47.6%)	133 (53.8%)
Focal (1%-10%)	63 (25.2%)	74 (30%)
Heterogeneous (11%-89%)	48 (19.2%)	17 (6.9%)
Diffuse (≥90%)	20 (8%)	23 (9.3%)
Characteristics of ILCs with diffuse E-cadherine expression		
E-cadherin H-score	241.7 (120-300)	209.6 (96-300)
Type of E-cadherin membrane staining:		
Continuous	3 (15%)	5 (21.7%)
Discontinuous	17 (85%)	18 (78.3%)

ILC, invasive lobular carcinoma.

Table 3
Characteristics of β-catenin and p120-catenin immunohistochemistry for the 19 cases with diffuse expression of E-cadherin (≥90%) with both clone 4A2C7 and NCH38

CDH1 status		β-catenin			p120-catenin			
		Membrane staining			Membrane staining			Cytoplasmic staining
		% of cells	Intensity	Type	% of cells	Intensity	Type	% of cells
CDH1 mutated ILCs	Extracellular domain	90	Weak	Incomplete	40	Moderate	Incomplete	10
		100	Strong	Incomplete	70	Moderate	Incomplete	1
		90	Moderate	Incomplete	90	Moderate	Incomplete	30
		95	Moderate	Incomplete	95	Strong	Incomplete	0
		90	Moderate	Incomplete	85	Moderate	Incomplete	5
		100	Moderate	Incomplete	90	Moderate	Incomplete	0
		100	Strong	Incomplete	100	Strong	Incomplete	0
		90	Moderate	Incomplete	90	Moderate	Incomplete	0
		100	Moderate	Incomplete	90	Moderate	Incomplete	0
		100	Strong	Complete	100	Strong	Complete	0
		100	Moderate	Incomplete	100	Moderate	Incomplete	0
		100	Moderate	Incomplete	80	Weak	Incomplete	60
	ICD	5	Weak	Incomplete	60	Weak	Incomplete	10
ILCs without *CDH1* mutation		70	Weak	Incomplete	40	Weak	Incomplete	10
		100	Moderate	Incomplete	70	Weak	Incomplete	10
		100	Moderate	Complete	100	Strong	Complete	0
		100	Strong	Incomplete	90	Moderate	Incomplete	0
		100	Strong	Incomplete	90	Strong	Incomplete	0
		100	Weak	Incomplete	85	Weak	Incomplete	5

ICD, intracellular domain; ILC, invasive lobular carcinoma.

E-cadherin had no fewer *CDH1* mutations than E-cadherin-negative cases but were significantly enriched in nontruncating mutations. In addition, for the first time to our knowledge, we showed that the presence of E-cadherin truncating mutations was associated with a higher risk of developing metastasis and a higher breast cancer-related mortality.

As some publications show discrepancies in E-cadherin IHC expression depending on the domain targeted by the antibody,[31] we performed IHC staining with 2 clones: clone NCH38 (which is the most used clone worldwide[5]) targeting the extracellular part of the protein and clone 4A2C7 targeting the intracellular domain. Although the results appeared more straightforward with

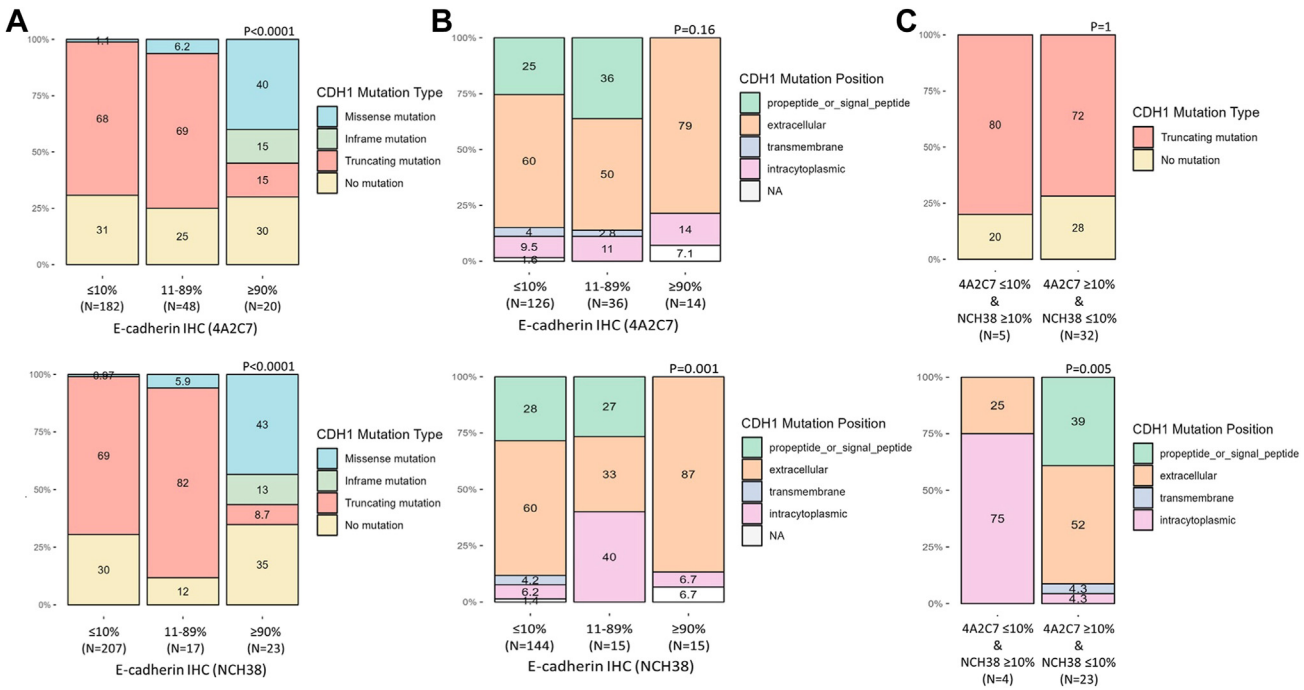

Figure 3.
Phenotypic correlation of *CDH1* mutations. Invasive lobular carcinomas with diffuse expression of E-cadherin (≥90%) are enriched in *CDH1* nontruncating mutations (A) and lack signal/propeptide domain mutations (B). A significant defect in E-cadherin expression with the intracellular clone (4A2C7 ≤ 10%), in conjunction with a conserved expression of E-cadherin with the extracellular clone (NCH38 ≥ 10%), is associated with enrichment in *CDH1* mutations of the intracytoplasmic domain (C).

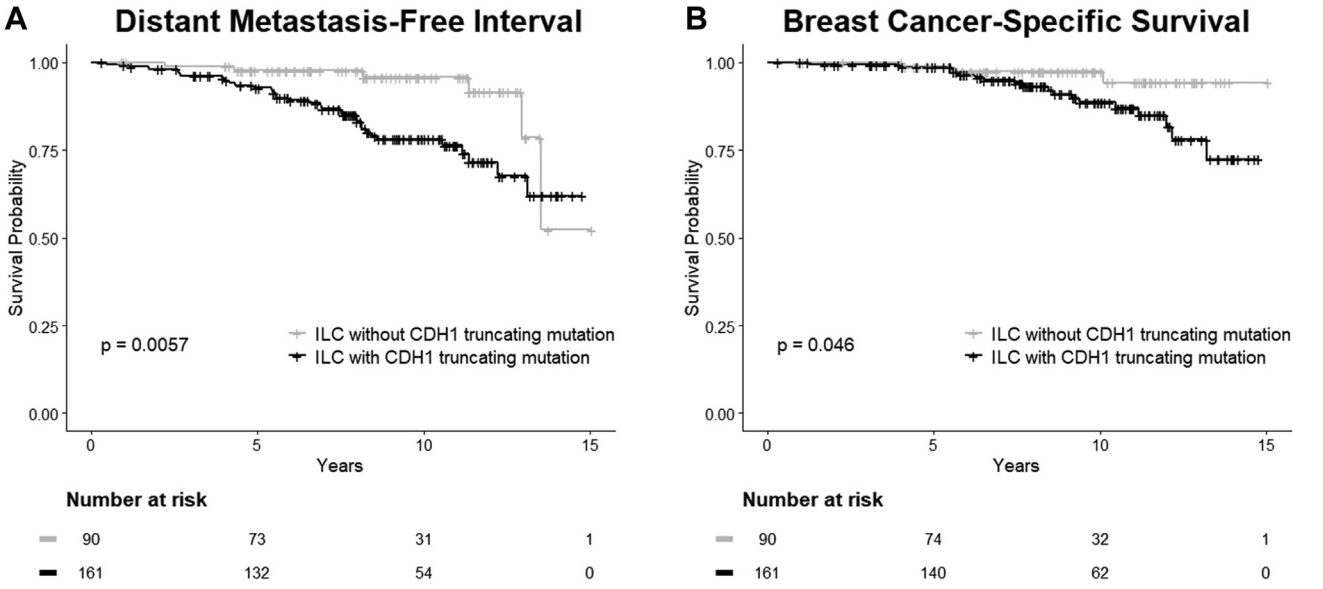

Figure 4.

CDH1 truncating mutations are associated with poor survival in invasive lobular carcinomas . Kaplan–Meier plots showing distant metastasis-free interval (A) and breast cancer-specific survival (B) of invasive lobular carcinomas patients stratified according to the absence (gray) or presence (black) of *CDH1* truncating mutation. The tables below the curves indicate the numbers of patients at risk.

clone NCH38 (usually null/focal or diffuse) than with clone 4A2C7 showing a higher proportion of heterogeneous staining (11%-89% of positive cells), the concordance between the 2 clones was still good when considering the 3 E-cadherin categories null/focal (≤10%) (72.8% for 4A2C7 vs 83.8% for NCH38), heterogeneous (11%-89%) (19.2% for 4A2C7 vs 6.9% for NCH38), and diffuse (≥90%) (8% for 4A2C7 vs 9.3% for NCH38) (overall concordance: 83.8%, Kappa 0.67). Importantly, E-cadherin expression, when present, was in almost all cases membranous and abnormal (incomplete and of reduced intensity compared with E-cadherin staining of normal glands). Although previous studies have been carried out with variable clones and E-cadherin positivity cutoffs, our results are in line with previously reported frequencies,[7,15] in particular, for the most studied clone NCH38.[14] Of note, nuclear expression of E-cadherin (which was not taken into account for the global assessment of percentage of labeled cells presented above) was seen with both clones and was anticorrelated with membrane E-cadherin expression, as found by Lobo and colleagues.[32]

Our study was based on *CDH1* mutation analysis from RNA sequencing data. This technique is routinely used in our institution for diagnostic purposes. This enables triple characterization (point mutations, fusion transcripts, and gene expression profile) from a single tumor fragment, which is particularly useful for small biopsies. *CDH1* being a tumor suppressor gene, we might have expected a lack of sensitivity for mutation detection by RNAseq. However, comparative DNA sequencing of 110 ILCs from our cohort demonstrated an excellent sensitivity (97.7%) of our RNA-based mutational analysis. In addition, the *CDH1* mutation rate in the entire series (70.5%) and the proportion of truncating *CDH1* mutation (89.5%) were close to those usually described in the literature,[4,10-13] supporting the reliability of our results.

Interestingly, we showed that cases with diffuse E-cadherin expression have the same *CDH1* mutation frequency (~70%) as cases with null/focal expression but differ significantly in mutation type. The association between retained E-cadherin expression and nontruncating *CDH1* mutations has been previously suggested, notably in a large series of *CDH1*-mutated breast cancer[33] and in a small series of ILC.[4] However, no genotype-phenotype correlation was provided in these series for ILC without a *CDH1* mutation. In our study, ILCs without *CDH1* mutation had typical morphologic features of lobular carcinomas, including 70% of classic histologic subtype and null/focal expression of E-cadherin (≤10%) in over 3-quarters of cases (similar to what we observe in ILCs with truncating *CDH1* mutation). The molecular mechanism of E-cadherin downregulation in ILCs without *CDH1* mutation is currently under investigation in our cohort, with recent reports showing that this may be primarily related to *CDH1* promoter methylation.[34]

In addition, we demonstrated an association between mutation location and E-cadherin protein expression. Signal/propeptide domain mutations were absent in ILCs with diffuse expression of E-cadherin (≥90%), and intracytoplasmic domain mutations were associated, as expected, with a divergent phenotype (intracellular clone 4A2C7 ≤10% and extracellular clone NCH38 ≥10%).

Our results may help standardize the diagnostic workup for ILCs with diffuse E-cadherin expression, which can be misleading to the pathologist. In our series, the morphology of these cases was clearly lobular, with the presence of a typical ILC morphology (dissociated isolated cells, single file pattern) and without features that would favor a mixed ductal/lobular form (absence of significant tube formation), although a minority of cases displayed trabecular, alveolar, or solid areas. Overall, the frequency of the classical histologic subtype was found to be similar or even higher in tumors with diffuse E-cadherin expression than in E-cadherin null/focal ILCs (70%-75% vs 64%-67%, respectively).

Based on our observations, the diagnosis of ILC could be supported in the rare cases with retained diffuse E-cadherin staining by (1) careful analysis of E-cadherin labeling (diffuse, but nearly always incomplete membrane labeling and reduced intensity compared with normal glands), (2) staining with another E-cadherin clone (17% of diffusely positive NCH38 cases in our series showed nondiffuse labeling with the intracellular 4A2C7 clone), (3) by β-catenin or p120-catenin staining (at least one antibody staining clearly abnormal in 21% of cases with diffuse E-cadherin in our series), and (4) by determining the *CDH1* gene mutational

Table 4
Univariate and multivariate Cox proportional hazards models for distant metastasis-free interval and breast cancer-specific survival.

Clinicopathological feature	Univariate analysis				Multivariate analysis			
	DMFI		BCSS		DMFI		BCSS	
	HR (95% CI)	*P* value	HR (95% CI)	*P* value	HR (95% CI)	*P* value	HR (CI 95%)	*P* value
Age (y)								
<50 (N = 53)	1		1					
50-64 (N = 104)	1.2 (0.47-2.8)	.75	2.7 (0.59-12)	.20				
≥65 (N = 94)	2.1 (0.85-5.0)	.11	3.9 (0.85-18)	.08				
Menopausal status								
Premenopausal (N = 72)	1		1					
Postmenopausal (N = 171)	1.2 (0.61-2.4)	.58	1.7 (0.64-4.8)	.27				
Histologic subtype								
Classic (N = 170)	1		1					
Nonclassic (N = 81)	1.8 (0.94-3.3)	.07	1.4 (0.57-3.3)	.48				
Apocrine morphology								
No (N = 237)	1		1					
Yes (N = 14)	1.6 (0.5-5.3)	.41	NA					
pT(m)								
Unifocal (N = 195)	1		1					
Multifocal (N = 56)	0.91 (0.42-2)	.81	1.1 (0.4-3)	.84				
Tumor Size								
pT1 (N = 154)	1		1		1		1	
pT2 (N = 76)	1.7 (0.86-3.5)	.12	1.9 (0.74-5)	.17	1.1 (0.53-2.3)	.79	1.09 (0.39-3.1)	.87
pT3 (N = 21)	4.0 (1.62-9.6)	.002[b]	3.9 (1.18-13)	.02[a]	1.0 (0.33-3.1)	.99	1.11 (0.24-5.2)	.89
Nodal status								
pN0 (N = 175)	1		1		1		1	
pN1 (N = 51)	1.7 (0.73-3.8)	.22	3.4 (1.2-9.3)	.01[a]	1.3 (0.54-3.1)	.57	2.33 (0.78-7.0)	.13
pN2 (N = 18)	7 (3.08-16)	<.001[c]	4.4 (1.1-17.3)	.03[a]	8.9 (3.48-22.5)	<.001[c]	5.48 (1.2-25.0)	.02[a]
pN3 (N = 7)	16.9 (6.04-47.1)	<.001[c]	19.6 (4.9-78.2)	<.001[c]	16.4 (4.82-55.5)	<.001[c]	21.82 (3.81-125)	<.001[c]
Grade								
1-2 (N = 214)	1		1		1		1	
3 (N = 37)	2.5 (1.2-5)	.01[a]	1.4 (0.47-4.2)	.54	2.2 (0.99-4.9)	.05	0.82 (0.24-2.8)	.75
Lymphovascular invasion								
No (N = 224)	1		1					
Yes (N = 27)	1.7 (0.77-3.9)	.18	1.8 (0.61-5.4)	.28				
Estrogen receptor								
Positive (N = 242)	1		1					
Negative (N = 9)	NA		NA					
Progesteron receptor								
Positive (N = 188)	1		1		1		1	
Negative (N = 63)	1.5 (0.75-2.9)	.25	2.4 (1-5.8)	.04[a]	1.44 (0.70-3.0)	.31	2.58 (1.02-6.5)	.04[a]
HER2								
HER2-zero (N = 160)	1		1					
HER2-low (N = 83)	1.4 (0.76-2.7)	.3	0.69 (0.25-1.9)	.46				
HER2-Positive (N = 8)	NA		NA					
Histomolecular class								
Luminal A (N = 171)	1		1					
Other subtypes (N = 80)	1.6 (0.87-3.1)	.12	2.1 (0.88-4.9)	.09				
Tumor infiltrating lymphocytes								
<5% (N = 182)	1		1		1		1	
≥5% (N = 69)	1.4 (0.75-2.8)	.27	2.4 (1-5.6)	.04[a]	1.7 (0.77-3.6)	.19	2.75 (1.00-7.6)	.05
Tumor cellularity								
<50% (N = 146)	1		1					
≥50% (N = 105)	1.1 (0.6-2.2)	.67	1.6 (0.66-3.8)	.28				
E-cadherin IHC (4A2C7)								
≤10% (N = 182)	1		1					
11-89% (N = 48)	0.41 (0.15-1.2)	.09	0.86 (0.29-2.6)	.79				
≥90% (N = 20)	0.49 (0.12-2.1)	.32	NA					
E-cadherin IHC (NCH38)								
≤10% (N = 207)	1		1					
11-89% (N = 17)	0.81 (0.19-3.4)	.77	1.67 (0.38-7.3)	.49				
≥90% (N = 23)	0.51 (1.12-2.1)	.35	0.53 (0.07-4)	.53				

(*continued on next page*)

Table 4 (*continued*)

Clinicopathological feature	Univariate analysis				Multivariate analysis			
	DMFI		BCSS		DMFI		BCSS	
	HR (95% CI)	*P* value	HR (95% CI)	*P* value	HR (95% CI)	*P* value	HR (CI 95%)	*P* value
CDH1 status								
No mutation (N = 74)	1		1		1		1	
Nontruncating mutation (N = 16)	2.3 (0.41-12)	.34	2.3 (0.21-25)	.50	2.8 (0.48-16.4)	.25	3.16 (0.27-37.5)	.36
Truncating mutation (N = 161)	3.9 (1.39-11)	.01[a]	4 (0.92-17)	.06	5.2 (1.72-15.7)	.003[b]	4.93 (1.06-23)	.04[a]
Surgery								
Tumorectomy (N = 168)	1		1					
Mastectomy (N = 83)	1.1 (0.57-2.2)	.75	1.5 (0.6-3.6)	.41				
Radiotherapy								
No (N = 22)	1		1					
Yes (N = 229)	3 (0.41-22)	.27	NA					
Chemotherapy								
No (N = 187)	1		1					
Yes (N = 64)	1.7 (0.87-3.2)	.12	1.5 (0.62-3.6)	.37				
Hormone therapy								
No (N = 35)	1		1					
Yes (N = 216)	1.1 (0.38-3)	.89	2.4 (0.32-18)	.38				

BCSS, breast cancer-specific survival; DMFI, distant metastasis-free interval; HR, hazard ratio; IHC, immunohistochemistry; NA, not assessable (no event in this category).
[a] $P < .05$.
[b] $P < .01$.
[c] $P < .001$.

status, given that *CDH1* mutations are present in a high proportion of such cases [65%-70%] (similar to the mutation rate observed in E-cadherin null/focal ILCs, but more often of the nontruncating type). The determination of *CDH1* mutation status for diagnostic purposes is currently not feasible in the routine practice of most laboratories. However, it may be considered in the near future in the context of the emergence of dedicated ILC therapies. Indeed, the reproducibility of ILC diagnosis is currently suboptimal,[2,3] and additional implementation of a molecular diagnostic test could potentially enable better identification of ILCs. Our data suggest that *CDH1* status may have both diagnostic utility (especially in those rare cases where morphologic and immunohistochemical analyses are insufficient for an accurate ILC diagnosis) and prognostic significance. Furthermore, larger studies are required to elucidate the precise added value of *CDH1* status assessment in ILC diagnosis and prognostic stratification.

Radiohistologic size discordance is one of the most striking distinctive features of infiltrating lobular carcinomas.[35] Indeed, in contrast to ductal carcinomas, the radiological size of lobular carcinomas (when assessed by mammography or ultrasound) frequently underestimates the effective histologic size of the tumor. We have shown that this clinicoradiological phenomenon is actually associated with the biological inactivation of *CDH1*, even in ILCs: lobular tumors with a truncating mutation of *CDH1* or null/focal expression of E-cadherin showed significantly more radiohistological size discordance than other cases. Furthermore, stromal content (inversely correlated with tumor cellularity) and TILs were less abundant in E-cadherin null/focal cases. These correlations call for further exploration of the biological effect of E-cadherin inactivation on stromal specificities in ILC (including TILs, cancer-associated fibroblast, and adipocyte content and function), in relation to the distinctive radiological characteristics of lobular carcinomas.[36]

Features usually associated with poor prognosis in ILC include tumor size, lymph node involvement, grade, tumor phenotype,[37–39] and TILs.[18,40] We show here for the first time to our knowledge that the presence of a *CDH1* truncating mutation is associated with a higher risk of metastasis and a higher breast cancer-related mortality, independently of other clinicopathological characteristics of ILC. Interestingly, the poor prognosis associated with truncating *CDH1* mutation was seen even when analyses were restricted to focal/null E-cadherin (IHC $\leq$10%), demonstrating the additive value of *CDH1* mutational status analysis on E-cadherin immunohistochemistry. In contrast, previous studies[10-12,39] have not reported a prognostic impact of *CDH1* mutations. This may be due to analyses being carried out on cohorts with more advanced disease (higher pT and pN stages)[11,12,39] than in our cohort and for some of them[12] with less patients and shorter follow-up. It could be also related to survival analyses that were performed without stratification on the truncating or nontruncating nature of *CDH1* mutations or to the use of different survival indicators.[11,39] In our study, we have used DMFI or BCSS to specifically reflect cancer-related metastatic events or death without undermining survival assessment by competing events (frequently occurring in this elderly population). The prognostic effect of the *CDH1* status found in our study must be interpreted in light of growing evidence that ILCs have an increased metastatic risk compared with ER+ invasive ductal carcinomas, particularly in long-term follow-up.[17,38,41] Therefore, our observation could directly link high metastatic risk not to lobular histology *per se,* but to the underlying biological inactivation of *CDH1* by truncating mutations. Insights could be provided by experiments thoroughly investigating different mechanisms of E-cadherin inactivation and their links with the biological processes of metastatic spread (tumor cell invasiveness, cell dormancy, stromal interactions, etc.).

In conclusion, our work showed the importance of the presence and type of *CDH1* mutations on the clinicoradiological, stromal, and phenotypic characteristics of ILC, as well as on the survival of the patients. Our findings contribute to a better understanding of the heterogeneity of lobular disease and could help refine diagnostic methods and criteria of ILC. Finally, if our results are confirmed in an independent series, it could lead researchers to systematically take *CDH1* mutation status and type into account in their future basic or clinical research on lobular carcinomas.

Acknowledgments

The authors would like to thank Khadidja Klouch and Andreia Goncalves for their technical support, the ICGex for sequencing support, and the European Lobular Breast Cancer Consortium (ELBCC). The authors also thank the Ruban Rose Association for funding RNAseq through their *Grand Prize* awarded to A.V.S.

Author Contributions

L.D., A.V.S., and F.M.G. designed the study. L.D. wrote and A.V.S. thoroughly reviewed the manuscript. L.F. provided the patient clinical data. L.D., A.B., L.F., M.C., and A.V.S. performed or interpreted immunohistochemical tests. C.B., G.P., J.M.P., V.R., L.F., A.B., and L.D. were responsible for molecular experiments and/or analysis. L.D., Y.K., and M.C. were involved in statistical analysis. A.V.S. and F.M.G. supervised the research. All authors critically revised the final version of the manuscript.

Data Availability

The data sets analyzed during the current study are available from the corresponding author on reasonable request.

Funding

A.V.S. received Ruban Rose Grant (*Grand Prize*) from Ruban Rose Association in 2012, which helped fund RNAseq sequencing of ILC samples.

Declaration of Competing Interest

F.C.B. received honoraria, travel support, and research grants from AstraZeneca and Daiichy-Sankyo. F.M.-G. received research support from Innate-Pharma, Roche, Institut Roche, and Bristol-Myers-Squibb (BMS). A.V.-S. received honoraria, travel support, and research grants from Daichi-Sankyo, AstraZeneca, MSD Avenir, Ibex Medical Analytics, Owkin, and Primaa.

Ethics Approval and Consent to Participate

This study was approved by the local ethics committee (Institut Curie Breast Cancer Group). Patients gave their informed consents for using tissue samples for research purposes available for all.

Supplementary Material

The online version contains supplementary material available at https://doi.org/10.1016/j.modpat.2024.100570.

References

1. WHO Classification of Tumours Editorial Board. *Breast Tumours*. 5th ed. International Agency for Research on Cancer; 2019.
2. Metzger O, Cardoso F, Poncet C, et al. Clinical utility of MammaPrint testing in Invasive Lobular Carcinoma: results from the MINDACT phase III trial. *Eur J Cancer*. 2020;138:S5–S6.
3. Christgen M, Gluz O, Harbeck N, et al. Differential impact of prognostic parameters in hormone receptor-positive lobular breast cancer. *Cancer*. 2020;126(22):4847–4858.
4. Christgen M, Kandt LD, Antonopoulos W, et al. Inter-observer agreement for the histological diagnosis of invasive lobular breast carcinoma. *J Pathol Clin Res*. 2022;8(2):191–205.
5. De Schepper M, Vincent-Salomon A, Christgen M, et al. Results of a worldwide survey on the currently used histopathological diagnostic criteria for invasive lobular breast cancer. *Mod Pathol*. 2022;35(12):1812–1820.
6. Christgen M, Steinemann D, Kühnle E, et al. Lobular breast cancer: clinical, molecular and morphological characteristics. *Pathol Res Pract*. 2016;212(7):583–597.
7. Christgen M, Cserni G, Floris G, et al. Lobular breast cancer: histomorphology and different concepts of a special spectrum of tumors. *Cancers (Basel)*. 2021;13(15):3695.
8. Van Baelen K, Geukens T, Maetens M, et al. Current and future diagnostic and treatment strategies for patients with invasive lobular breast cancer. *Ann Oncol*. 2022;33(8):769–785.
9. Bergeron A, MacGrogan G, Bertaut A, et al. Triple-negative breast lobular carcinoma: a luminal androgen receptor carcinoma with specific ESRRA mutations. *Mod Pathol*. 2021;34(7):1282–1296.
10. Ciriello G, Gatza ML, Beck AH, et al. Comprehensive molecular portraits of invasive lobular breast cancer. *Cell*. 2015;163(2):506–519.
11. Desmedt C, Zoppoli G, Gundem G, et al. Genomic characterization of primary invasive lobular breast cancer. *J Clin Oncol*. 2016;34(16):1872–1881.
12. Michaut M, Chin S-F, Majewski I, et al. Integration of genomic, transcriptomic and proteomic data identifies two biologically distinct subtypes of invasive lobular breast cancer. *Sci Rep*. 2016;6:18517.
13. McCart Reed AE, Kalinowski L, Simpson PT, Lakhani SR. Invasive lobular carcinoma of the breast: the increasing importance of this special subtype. *Breast Cancer Res*. 2021;23(1):6.
14. Rakha EA, Patel A, Powe DG, et al. Clinical and biological significance of E-cadherin protein expression in invasive lobular carcinoma of the breast. *Am J Surg Pathol*. 2010;34(10):1472–1479.
15. Canas-Marques R, Schnitt SJ. E-cadherin immunohistochemistry in breast pathology: uses and pitfalls. *Histopathology*. 2016;68(1):57–69.
16. Bajrami I, Marlow R, van de Ven M, et al. E-cadherin/ROS1 inhibitor synthetic lethality in breast cancer. *Cancer Dis*. 2018;8(4):498–515.
17. Djerroudi L, Cabel L, Bidard F-C, Vincent-Salomon A. Invasive lobular carcinoma of the breast: toward tailoring therapy? *J Natl Cancer Inst*. 2022;114(11):1434–1436.
18. Tille J-C, Vieira AF, Saint-Martin C, et al. Tumor-infiltrating lymphocytes are associated with poor prognosis in invasive lobular breast carcinoma. *Mod Pathol*. 2020;33(11):2198–2207.
19. Wolff AC, Hammond MEH, Allison KH, et al. Human epidermal growth factor receptor 2 testing in breast cancer: American Society of Clinical Oncology/College of American Pathologists Clinical Practice guideline focused update. *J Clin Oncol*. 2018;36(20):2105–2122.
20. Allison KH, Hammond MEH, Dowsett M, et al. Estrogen and progesterone receptor testing in breast cancer: American Society of Clinical Oncology/College of American Pathologists guideline update. *Arch Pathol Lab Med*. 2020;144(5):545–563.
21. Franchet C, Djerroudi L, Maran-Gonzalez A, et al. [2021 update of the GEFPICS' recommendations for HER2 status assessment in invasive breast cancer in France]. *Ann Pathol*. 2021;41(6):507–520.
22. Balaton AL, Coindre JM, Collin F, et al. [Recommendations for the immunohistochemical evaluation of hormone receptors on paraffin sections of breast cancer. Study Group on Hormone Receptors using Immunohistochemistry FNCLCC/AFAQAP. National Federation of Centres to Combat Cancer/French Association for Quality Assurance in Pathology]. *Ann Pathol*. 1996;16(2):144–148.
23. Zafrani B, Aubriot MH, Mouret E, et al. High sensitivity and specificity of immunohistochemistry for the detection of hormone receptors in breast carcinoma: comparison with biochemical determination in a prospective study of 793 cases. *Histopathology*. 2000;37(6):536–545.
24. Goldhirsch A, Wood WC, Coates AS, et al. Strategies for subtypes–dealing with the diversity of breast cancer: highlights of the St. Gallen International Expert Consensus on the Primary Therapy of Early Breast Cancer 2011. *Ann Oncol*. 2011;22(8):1736–1747.
25. Amin M. *AJCC Cancer Staging Manual*. 8th ed. Springer; 2018.
26. Robinson JT, Thorvaldsdóttir H, Winckler W, et al. Integrative genomics viewer. *Nat Biotechnol*. 2011;29(1):24–26.
27. Kopanos C, Tsiolkas V, Kouris A, et al. VarSome: the human genomic variant search engine. *Bioinformatics*. 2019;35(11):1978–1980.
28. Villy M-C, Masliah-Planchon J, Buecher B, et al. Endometrial cancer may be part of the MUTYH-associated polyposis cancer spectrum. *Eur J Med Genet*. 2022;65(1):104385.
29. Chakravarty D, Gao J, Phillips S, et al. OncoKB: a precision oncology knowledge base. *JCO Precis Oncol*. 2017;(1):1–16.
30. Suehnholz SP, Nissan MH, Zhang H, et al. Quantifying the expanding landscape of clinical actionability for patients with cancer. *Cancer Discov*. 2024;14(1):49–65.
31. Yasui H, Kawata T, Muramatsu K, et al. Expression of N-terminal-deficient E-cadherin protein in invasive lobular carcinoma of the breast. *Am J Surg Pathol*. 2022;46(3):383–391.
32. Lobo J, Petronilho S, Newell AH, et al. E-cadherin clone 36 nuclear staining dictates adverse disease outcome in lobular breast cancer patients. *Mod Pathol*. 2019;32(11):1574–1586.

33. Grabenstetter A, Mohanty AS, Rana S, et al. E-cadherin immunohistochemical expression in invasive lobular carcinoma of the breast: correlation with morphology and CDH1 somatic alterations. *Hum Pathol*. 2020;102:44–53.
34. Derakhshan F, Dopeso H, Paula ADC, et al. Abstract PD14-03: genetic and epigenetic basis of invasive lobular carcinomas lacking CDH1-alterations. *Cancer Res*. 2022;82(4_Supplement). PD14-03.
35. Boetes C, Mus RD, Holland R, et al. Breast tumors: comparative accuracy of MR imaging relative to mammography and US for demonstrating extent. *Radiology*. 1995;197(3):743–747.
36. Johnson K, Sarma D, Hwang ES. Lobular breast cancer series: imaging. *Breast Cancer Res*. 2015;17(1):94.
37. Arpino G, Bardou VJ, Clark GM, Elledge RM. Infiltrating lobular carcinoma of the breast: tumor characteristics and clinical outcome. *Breast Cancer Res*. 2004;6(3):R149–R156.
38. Rakha EA, El-Sayed ME, Powe DG, et al. Invasive lobular carcinoma of the breast: response to hormonal therapy and outcomes. *Eur J Cancer*. 2008;44(1):73–83.
39. McCart Reed AE, Foong S, Kutasovic JR, et al. The genomic landscape of lobular breast cancer. *Cancers*. 2021;13(8):1950.
40. Desmedt C, Salgado R, Fornili M, et al. Immune infiltration in invasive lobular breast cancer. *J Natl Cancer Inst*. 2018;110(7):768–776.
41. Oesterreich S, Nasrazadani A, Zou J, et al. Clinicopathological features and outcomes comparing patients with invasive ductal and lobular breast cancer. *J Natl Cancer Inst*. 2022;114(11):1511–1522.